

Supplementary Information

Title: Supramolecular temperature responsive assembly of polydopamine reduced graphene oxide

*Yiwen Chen, Thomas Szkopek, and Marta Cerruti\**

Table S1. Summary of synthesis conditions used so far to create PNIPAM-modified graphene/GO/rGO

The methods are classified in two categories, depending on if in the resulting material PNIPAM was bound covalently or non-covalently to the graphene-based substrates.

Abbreviations:

THF: tetrahydrofuran

CTA: chain transfer agent

RAFT: reversible addition fragmentation chain transfer

ATRP: atom transfer radical polymerization

DMF: dimethylformamide

SET-LRP: single electron transfer-living radical polymerization

ATNRC: atom transfer nitroxide radical coupling

AIBN: 2,2'-Azobis(2-methylpropionitrile)

APS: ammonium persulfate

TEMPO: 2,2,6,6-tetramethylpiperidine-1-oxyl

PNIPAM grafted graphene, GO or rGO	Polymerization type	Synthesis steps	Temperature (°C)	Solvent	Atmosphere	Purification steps
Non-covalent binding						
graphene/PNIPAM <sup>1</sup>	RAFT	1) Synthesis of pyrene-terminated RAFT CTA; 2) synthesis of pyrene terminated PNIPAM via RAFT; 3) adsorption of PNIPAM on graphene	65	THF	N <sub>2</sub>	column chromatography; vacuum evaporation; filtration; precipitating cycles; freeze-drying; centrifugation cycles
GO/PNIPAM <sup>2</sup>	ATRP	1) synthesis of perylene functionalized ATRP initiator; 2) polymerization of NIPAM via ATRP to obtain perylene modified PNIPAM;	0-60	isopropanol ethanol; THF	N <sub>2</sub>	column chromatography; washing; vacuum evaporation; rotary evaporation; precipitating cycles;

		3) adsorption of PNIPAM on GO				centrifugation cycles
rGO/PNIPAM <sup>3</sup>	free radical polymerization	1) synthesis of ionic liquid monomer; 2) co-polymerization of NIPAM and ionic liquid; 3) reduction of GO and adsorption of PNIPAM on rGO via cation- $\pi$ coupling	25-100	methanol	Ar	filtration; vacuum evaporation; precipitating cycles; dialysis; freeze-drying centrifugation
Covalent method						
graphene/PNIPAM <sup>4</sup>	ATRP	1) synthesis of OH- and Br-terminated graphene as ATRP initiator; 2) NIPAM polymerization on graphene via ATRP	0-80	DMF; water	N <sub>2</sub>	filtration; washing; vacuum evaporation
GO/PNIPAM <sup>5</sup>	click chemistry	1) synthesis of alkynyl-GO; 2) polymerization of NIPAM and synthesis of azide-terminated PNIPAM; 3) grafting of PNIPAM on graphene via click chemistry	25-45	DMF; THF	Ar	filtration; column chromatography; vacuum evaporation; centrifugation; precipitating cycles; freeze-drying; dialysis
GO/PNIPAM <sup>6</sup>	SET-LRP	1) synthesis of OH-terminated GO; 2) synthesis of Br-terminated GO as SET-LRP initiator; 3) polymerization of NIPAM on GO via SET-LRP	0-25	DMF; water	N <sub>2</sub>	filtration; washing; column chromatography; precipitating cycles; vacuum evaporation
GO/PNIPAM <sup>7</sup>	ATRP	1) synthesis of OH- and Br-terminated graphene; 2) NIPAM polymerization on graphene via ATRP	0-65	CHCl <sub>3</sub> , ethanol	Ar	filtration cycles; washing; vacuum evaporation
GO/PNIPAM <sup>8</sup>	free radical polymerization	1) freeze-pump-thaw for NIPAM monomer; 2) polymerization of NIPAM,	65	DMF	N <sub>2</sub>	centrifugations; washing; dialysis; freeze-drying

		grafting to double-bond sites on GO, initiated by AIBN				
GO/PNIPAM <sup>9</sup>	free radical polymerization	1) freeze-pump-thaw for NIPAM monomer; 2) polymerization of NIPAM, grafting to double-bond sites on GO, initiated by AIBN	65	DMF	N <sub>2</sub>	centrifugations; washing; dialysis; freeze-drying
GO/PNIPAM <sup>10</sup>	free radical polymerization	1) synthesis of GO-based initiator via nucleophilic ring-opening reaction; 2) polymerization of NIPAM on GO	70-80	water	N <sub>2</sub>	centrifugations; washing cycles; dialysis
GO/PNIPAM <sup>11</sup>	free radical polymerization	1) re-crystallization of NIPAM in hexane twice; 2) oxygen removal; 3) polymerization of NIPAM initiated by APS, and grafting to GO through ether bonding	75	water	Ar	filtration; washing cycles; vacuum evaporation
GO/PNIPAM <sup>12</sup>	redox polymerization	ammonium cerium (IV) nitrate as initiator, polymerization of NIPAM	50	water	N <sub>2</sub>	centrifugations; washing cycles; vacuum evaporation
rGO/PNIPAM <sup>13</sup>	SET-LRP and ATNRC	1) freeze-pump-thaw for monomer; 2) synthesis of Cl-terminated GO; 3) reduction of GO and synthesis of coupling agent rGO/TEMPO; 4) SET-LRP synthesis of Br-terminated PNIPAM; 5) ATNRC synthesis of rGO/PNIPAM	0-70	DMF; THF	N <sub>2</sub>	column chromatography; centrifugation; precipitating cycles; filtration; washing cycles; vacuum evaporation
rGO/PNIPAM <sup>14</sup>	click chemistry and RAFT	1) synthesis of alkyne-terminated rGO; 2) synthesis RAFT CTA;	-30-60	acetonitrile; DMF; water; methanol	N <sub>2</sub>	column chromatography; filtration; centrifugation cycles;

		3) grafting CTA on rGO via click chemistry; 4) NIPAM polymerization on rGO via RAFT				washing cycles; vacuum evaporation
--	--	---	--	--	--	------------------------------------

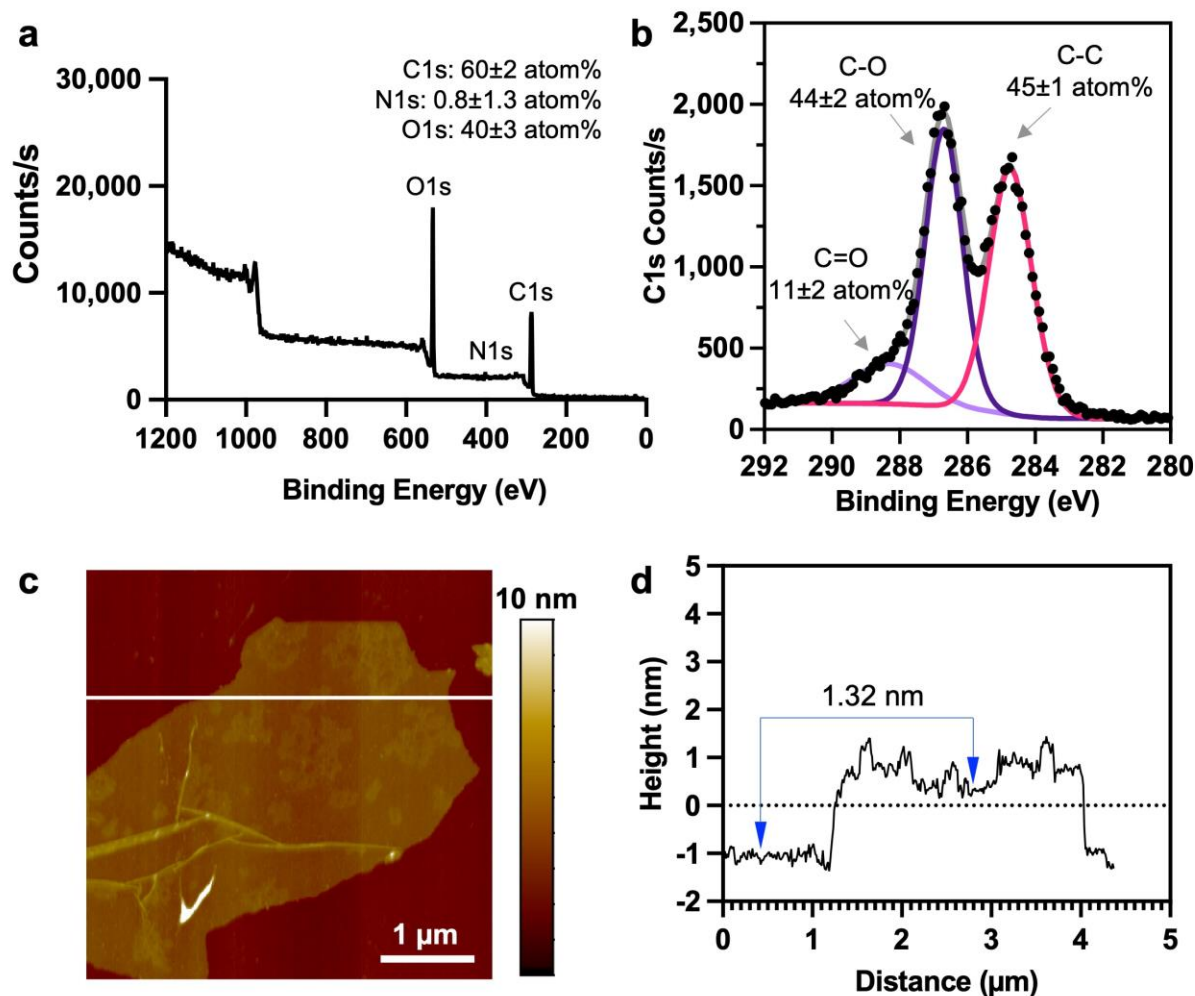


Fig. S1. Representative XPS (a) survey and (b) high resolution C1s spectra of pristine GO. The numbers shown in the figures display the atomic percentage of C1s, N1s, O1s from survey scans, and C-C, C-O, C=O atomic percentage from high resolution C1s scans. Nitrogen is an impurity deriving from sodium nitrate used in the Hummers' method for GO preparation. (c) AFM topography of a GO flake and (d) height profile corresponding to the cross section along the white line in panel (c).

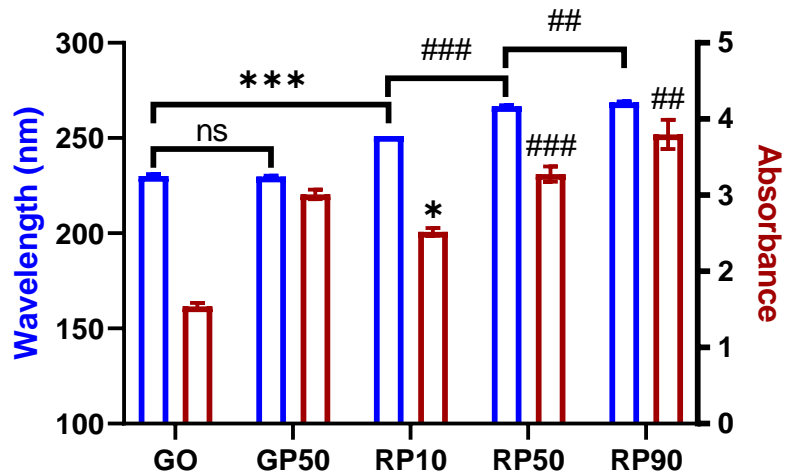


Fig. S2. Wavelength and corresponding maximum absorbance of the  $\pi$ - $\pi^*$  transition peaks from UV-vis spectrophotometry data of GO, GP, and RP (concentration 0.05 mg/mL). ns: no significant difference between GO and GP50 ( $P \geq 0.05$ ). \*\*\* and \*: significant difference between GO and RP10 (\*\*\* $P < 0.001$ , \* $P < 0.05$ ). ## and ###: significant difference between RP10 and RP50, RP50 and RP90 (## $P < 0.01$ , ### $P < 0.001$ ).

Table S2. Surface composition derived from XPS survey data of RP and GP (n=3). C1s and O1s amounts were not compared because GO, rGO and PDA both contribute to these elements.

	RP10	RP50	RP90	GP50
C1s (atom%)	72.7±0.3	77.8±0.4	71.5±0.1	68.9±0.5
O1s (atom%)	24.4±0.4	17.5±0.1	23.0±0.2	27.4±0.1
N1s (atom%)	3.0±0.1	4.6±0.2***	5.5±0.2##	3.8±0.4

\*\*\* and ##: significant difference between RP10 and RP50 or between RP50 and RP90 (## $P < 0.01$ , \*\*\* $P < 0.001$ ).

Table S3. Atom % obtained from the deconvolution of high resolution XPS C1s spectra of RP and GP (n=3 experiment points). Statistical analysis for atom% of C-N, C-O and C=O is shown in Figure 1.

	GO	RP10	RP50	RP90	GP50
C-C (atom%)	45±1	48.1±0.3	53.1±0.4	49±1	45±3
C-N (atom%)	--	10.3±0.4	12.4±0.6	15.8±0.3	9±1
C-O (atom%)	44±2	29.0±0.5	19.3±0.8	18.0±0.4	37±3
C=O (atom%)	11±2	11.1±0.4	13±1	15.0±0.5	8.2±0.2

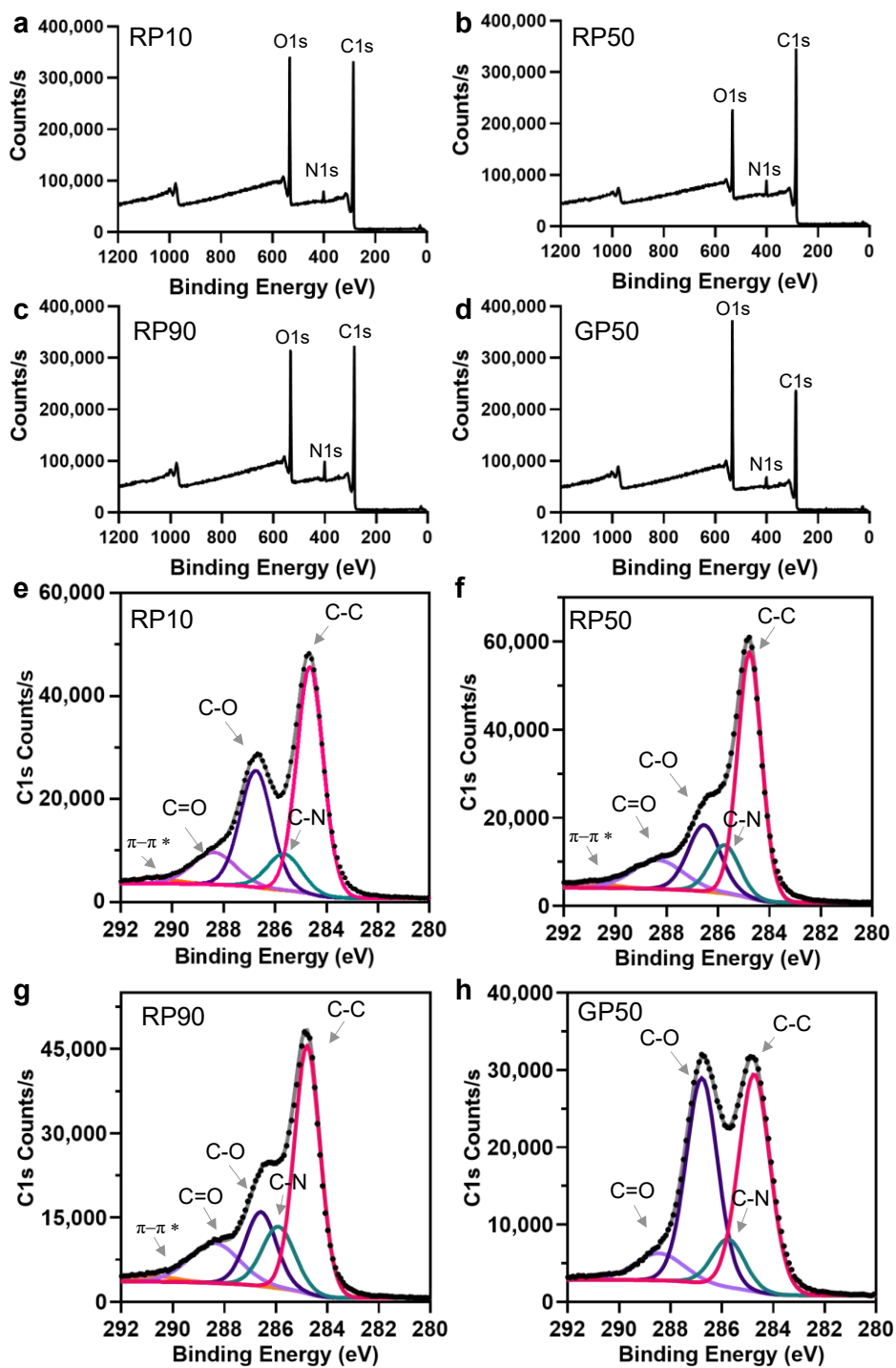


Fig. S3. Representative XPS survey (a-c) and high resolution C1s spectra (e-h) of rGO/PDA: (a, e) RP10, (b, f) RP50, (c, g) RP90, and GO/PDA: (d, h) GP50.

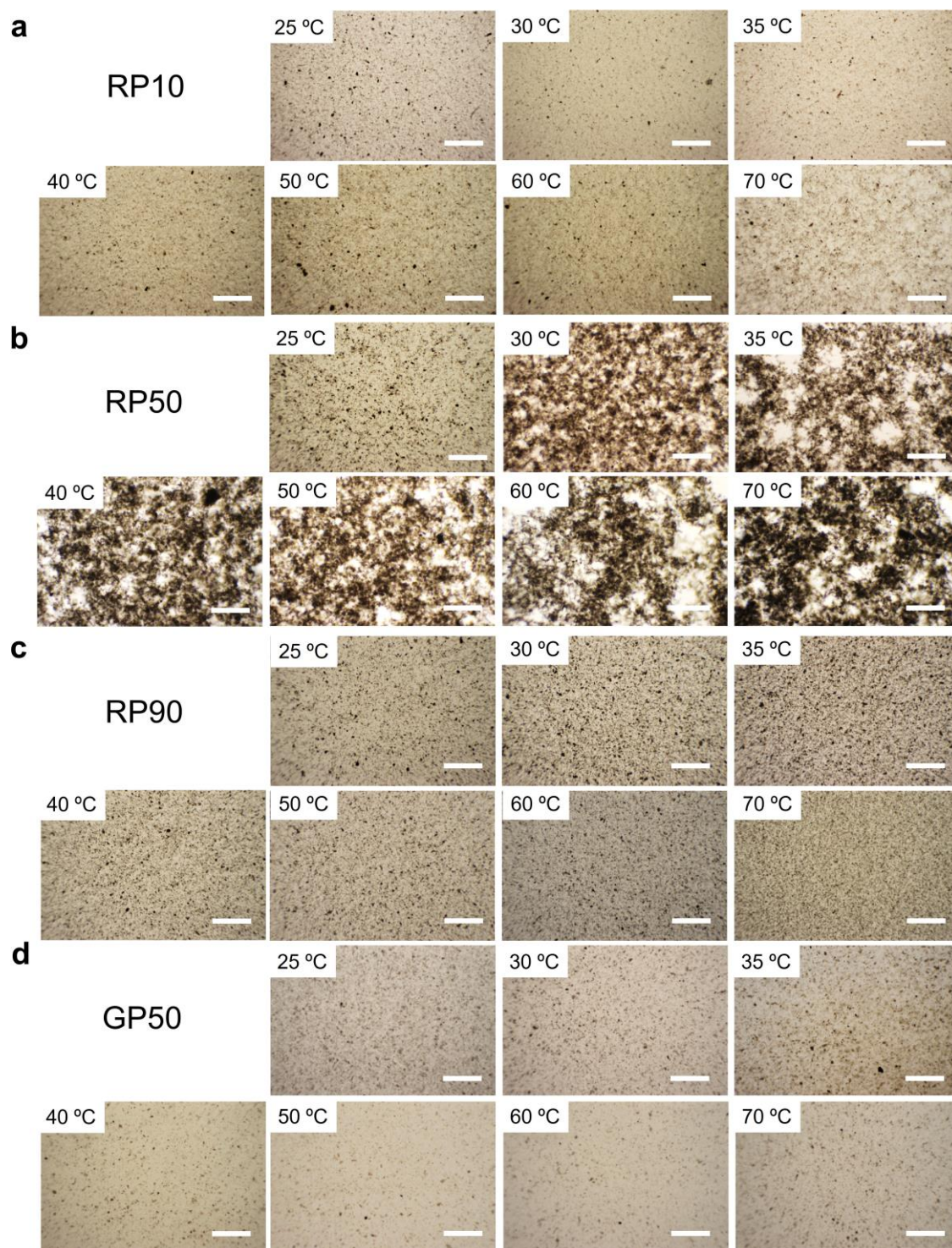


Fig. S4. Optical microscopy images of (a) RP10, (b) RP50, (c) RP90 and (d) GP50, at different temperatures. Scale bars = 500  $\mu\text{m}$  in all panels.

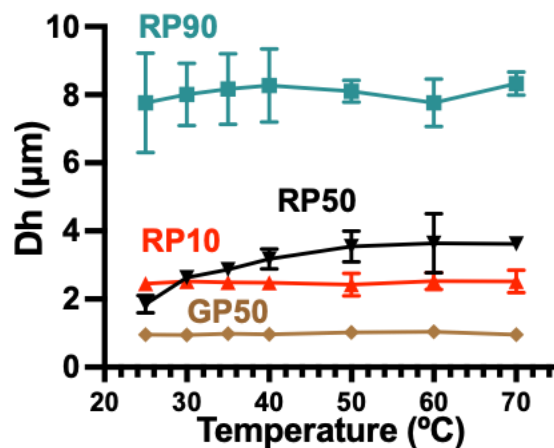


Fig. S5. Hydrodynamic diameter  $D_h$  of RP10, RP50, RP90 and GP50 after maintaining the indicated temperatures for 30 mins. There are  $n = 3$  independent experiments. The data are represented as mean  $\pm$  standard deviation.

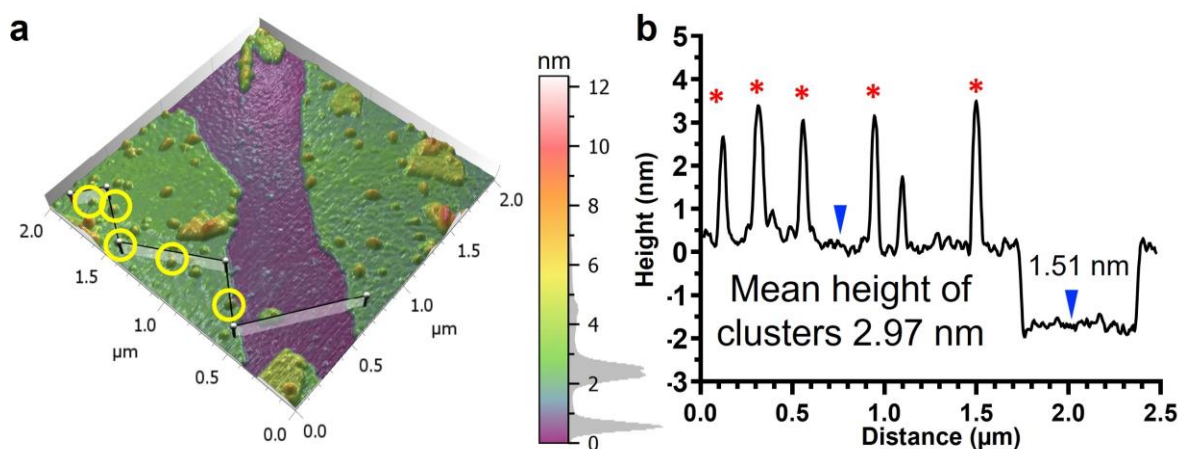


Fig. S6. (a) 3D AFM topography image of RP50 with corresponding histogram distribution of counts vs height. Representative PDA clusters are circled in yellow. (b) Height profile corresponding to the line in panel (a). The peaks indicated by red asterisks show the height of PDA clusters in panel (a). The height difference (1.51 nm) between blue arrows represents the height difference between RP50 flake (shown as green in panel a) and the substrate (shown as purple in panel a).

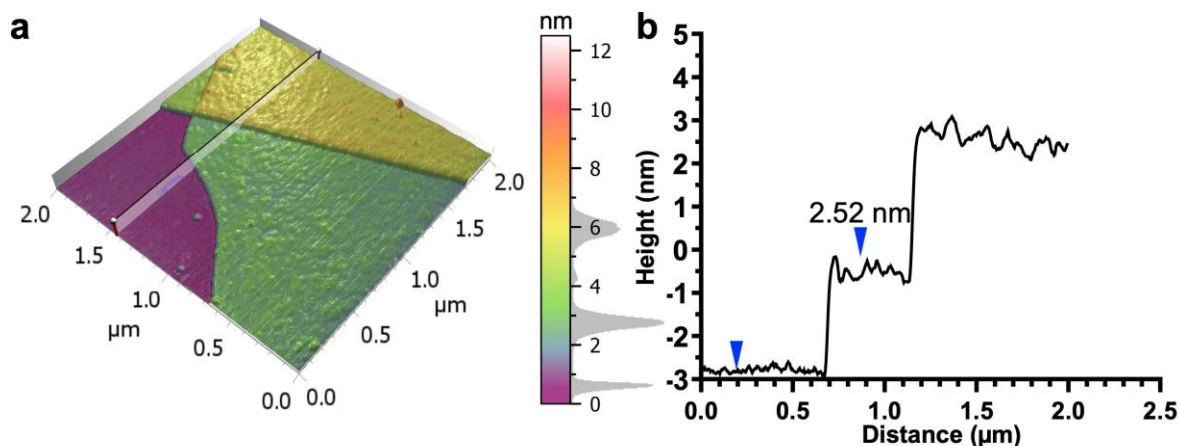


Fig. S7. (a) 3D AFM topography image of RP90 with corresponding histogram distribution of counts vs height. (b) Height profile corresponding to the line in panel (a).

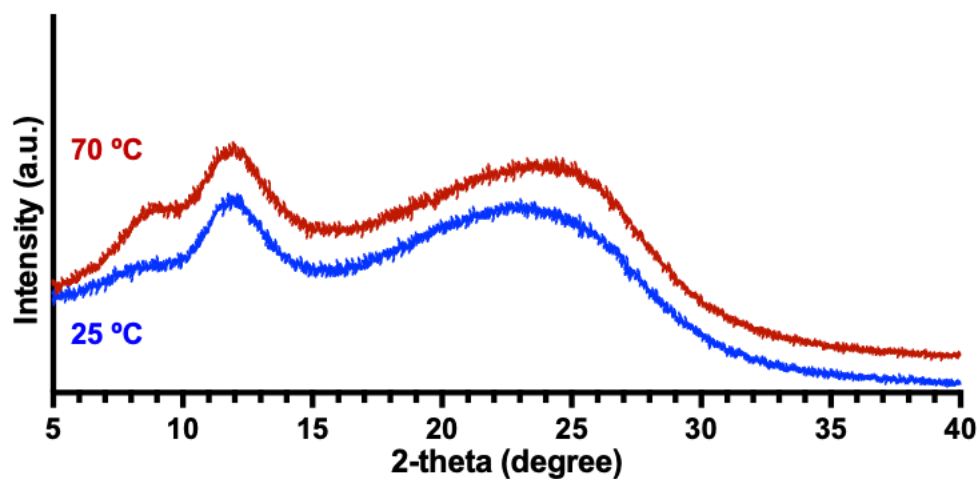


Fig. S8. XRD diffraction patterns of films prepared from RP50 at 25°C (bottom) and 70°C (top). The broad diffraction peaks at 2-theta  $\sim$  8° indicate an expansion of the interlayer spacing due to the incorporation of PDA between layers.<sup>15,16</sup> The broad peaks at 2-theta  $\sim$  12° indicate an expansion due to the presence of oxygen-containing groups on the rGO attached between layers.<sup>17</sup> The rest broad peaks are assigned to the (0 0 2) graphitic diffraction order typical of rGO.<sup>18,19</sup>

#### References:

- 1J. Liu, W. Yang, L. Tao, D. Li, C. Boyer and T. P. Davis, *J. Polym. Sci., Part A: Polym. Chem.*, 2010, **48**, 425–433.
- 2L. Wang, L. Jiang, D. Su, C. Sun, M. Chen, K. Goh and Y. Chen, *J. Colloid Interface Sci.*, 2014, **430**, 121–128.

- 3 Q. Zhang, J. Zhang, B. Liu, L. Zhang, L. Dong, E. Li, H. Zhang and L. Xia, *Chem. Commun.*, 2017, **53**, 6367–6370.
- 4 L. Ren, S. Huang, C. Zhang, R. Wang, W. W. Tjiu and T. Liu, *J. Nanopart. Res.*, 2012, **14**, 940.
- 5 Y. Pan, H. Bao, N. G. Sahoo, T. Wu and L. Li, *Adv. Funct. Mater.*, 2011, **21**, 2754–2763.
- 6 Y. Deng, J. Z. Zhang, Y. Li, J. Hu, D. Yang and X. Huang, *J. Polym. Sci., Part A: Polym. Chem.*, 2012, **50**, 4451–4458.
- 7 S. Zhu, J. Li, Y. Chen, Z. Chen, C. Chen, Y. Li, Z. Cui and D. Zhang, *J. Nanopart. Res.*, 2012, **14**, 1132.
- 8 J. Liu, L.-J. Yu, G. Yue, N. Wang, Z. Cui, L. Hou, J. Li, Q. Li, A. Karton, Q. Cheng, L. Jiang and Y. Zhao, *Adv. Funct. Mater.*, 2019, **29**, 1808501.
- 9 J. Liu, N. Wang, L.-J. Yu, A. Karton, W. Li, W. Zhang, F. Guo, L. Hou, Q. Cheng, L. Jiang, D. A. Weitz and Y. Zhao, *Nat. Commun.*, 2017, **8**, 2011.
- 10 H. Zhang, Q. Zhang, L. Zhang, T. Pei, E. Li, H. Wang, Q. Zhang and L. Xia, *Chem. – Eur. J.*, 2019, **25**, 1535–1542.
- 11 J. Zhu, X. Ding, D. Li, M. Dou, M. Lu, Y. Li and F. Luo, *ACS Appl. Mater. Interfaces*, 2019, **11**, 16443–16451.
- 12 B. Wang, D. Yang, J. Z. Zhang, C. Xi and J. Hu, *J. Phys. Chem. C*, 2011, **115**, 24636–24641.
- 13 Y. Deng, Y. Li, J. Dai, M. Lang and X. Huang, *J. Polym. Sci., Part A: Polym. Chem.*, 2011, **49**, 1582–1590.
- 14 Y. Yang, X. Song, L. Yuan, M. Li, J. Liu, R. Ji and H. Zhao, *J. Polym. Sci., Part A: Polym. Chem.*, 2012, **50**, 329–337.
- 15 W. Cui, M. Li, J. Liu, B. Wang, C. Zhang, L. Jiang and Q. Cheng, *ACS Nano*, 2014, **8**, 9511–9517.
- 16 R. Zou, F. Liu, N. Hu, H. Ning, X. Jiang, C. Xu, S. Fu, Y. Li, X. Zhou and C. Yan, *Carbon*, 2019, **149**, 173–180.
- 17 K. Krishnamoorthy, M. Veerapandian, K. Yun and S.-J. Kim, *Carbon*, 2013, **53**, 38–49.
- 18 L. Stobinski, B. Lesiak, A. Malolepszy, M. Mazurkiewicz, B. Mierzwa, J. Zemek, P. Jiricek and I. Bielowshapka, *J. Electron Spectrosc. Relat. Phenom.*, 2014, **195**, 145–154.
- 19 S. Park, J. An, J. R. Potts, A. Velamakanni, S. Murali and R. S. Ruoff, *Carbon*, 2011, **49**, 3019–3023.